Monthly Notices
of the
ROYAL ASTRONOMICAL SOCIETY

MNRAS **433,** 1764–1777 (2013)
Advance Access publication 2013 June 7

doi:10.1093/mnras/stt850

A high Eddington-ratio, true Seyfert 2 galaxy candidate: implications for broad-line region models

G. Miniutti,[1]⋆ R. D. Saxton,[2] P. M. Rodríguez-Pascual,[2] A. M. Read,[3] P. Esquej,[1,4,5] M. Colless,[6] P. Dobbie[6,7] and M. Spolaor[6]

[1]*Centro de Astrobiología (CSIC-INTA), Dep. de Astrofísica; ESAC, PO Box 78, E-28691 Villanueva de la Cañada, Madrid, Spain*
[2]*XMM SOC, ESAC, PO Box 78, E-28691, Villanueva de la Cañada, Madrid, Spain*
[3]*Department of Physics and Astronomy, University of Leicester, Leicester LE1 7RH, UK*
[4]*Instituto de Física de Cantabria, CSIC-Universidad de Cantabria, 39005 Santander, Spain*
[5]*Departamento de Física Moderna, Universidad de Cantabria, Avda. de Los Castros s/n, 39005 Santander, Spain*
[6]*Australian Astronomical Observatory, PO Box 915, North Ryde, NSW 1670, Australia*
[7]*School of Maths and Physics, University of Tasmania, Sandy Bay 7001, Australia*

Accepted 2013 May 14. Received 2013 May 13; in original form 2012 November 27

ABSTRACT

A bright, soft X-ray source was detected on 2010 July 14 during an *XMM–Newton* slew at a position consistent with the galaxy GSN 069 ($z = 0.018$). Previous *ROSAT* observations failed to detect the source and imply that GSN 069 is now $\geq$240 times brighter than it was in 1994 in the soft X-ray band. Optical spectra (from 2001 to 2003) are dominated by unresolved emission lines with no broad components, classifying GSN 069 as a Seyfert 2 galaxy. We report here results from a $\sim$1 yr monitoring with *Swift* and *XMM–Newton*, as well as from new optical spectroscopy. GSN 069 is an unabsorbed, ultrasoft source in X-rays, with no flux detected above $\sim$1 keV. The soft X-rays exhibit significant variability down to time-scales of hundreds of seconds. The UV-to-X-ray spectrum of GSN 069 is consistent with a pure accretion disc model which implies an Eddington ratio $\lambda \simeq 0.5$ and a black hole mass of $\simeq 1.2 \times 10^6\,M_\odot$. A new optical spectrum, obtained $\sim$3.5 months after the *XMM–Newton* slew detection, is consistent with earlier spectra and lacks any broad-line component. The lack of cold X-ray absorption and the short time-scale variability in the soft X-rays rule out a standard Seyfert 2 interpretation of the source. The present Eddington ratio of GSN 069 exceeds the critical value below which no emitting broad-line region (BLR) forms, according to popular models, so that GSN 069 can be classified as a bona-fide high Eddington-ratio true Seyfert 2 galaxy. We discuss our results within the framework of two possible scenarios for the BLR in AGN, namely the two-phase model (cold BLR clouds in pressure equilibrium with a hotter medium), and models in which the BLR is part of an outflow, or disc-wind. Finally, we point out that GSN 069 may be a member of a population of super-soft active galactic nuclei (AGN) whose spectral energy distribution is completely dominated by accretion disc emission, as it is the case in some black hole X-ray binary transients during their outburst evolution. The disc emission for a typical AGN with black hole mass of 10^7–$10^8\,M_\odot$ does not enters the soft X-ray band, so that GSN 069-like objects with larger black hole mass (i.e. the bulk of the AGN population) are missed by current X-ray surveys, or misclassified as Compton-thick candidates. If the analogy between black hole X-ray binary transients and AGN holds, the lifetime of these super-soft states in AGN may be longer than 10^4 years, implying that the actual population of super-soft AGN may not be negligible, possibly contaminating the estimated fraction of heavily obscured AGN from current X-ray surveys.

Key words: accretion, accretion discs – galaxies: active – galaxies: Seyfert – X-rays: galaxies.

1 INTRODUCTION

One of the key ideas upon which we base our understanding of active galactic nuclei (AGN) is that type 1 and type 2 AGN have

⋆E-mail: gminiutti@cab.inta-csic.es

no intrinsic physical differences, their classification being dominated by the presence/absence of absorbing material in our line of sight (LOS), which is considered to be orientation dependent (Antonucci 1993; see also Elitzur 2012). Although this Unified Model has been extremely successful, additional ingredients are likely needed to account for some observational facts that apparently are in conflict with the expectations. Among these, it is well known that a significant fraction of the brightest Seyfert 2 galaxies lack broad optical lines even in polarized light (e.g. Tran 2003). Moreover, a (still relatively small) sample of Seyfert 2 galaxies have been found to be unabsorbed in the X-rays, thus challenging the Unified Model (Pappa et al. 2001; Panessa & Bassani 2002; Brightman & Nandra 2008; Panessa et al. 2009; Shi et al. 2010; Bianchi et al. 2012, but see Antonucci 2012 for a series of motivated caveats).

Various explanations have been proposed to solve the apparent puzzle of unabsorbed Seyfert 2 galaxies. The proposed explanations range from dilution (the broad, optical lines can be overwhelmed by the host galaxy contribution) to large amplitude, long-term variability (either in luminosity or in absorption properties) and signal-to-noise issues. However, good signal-to-noise optical and quasi-simultaneous X-ray data seem to point towards the real existence of a population of genuine unabsorbed Seyfert 2 galaxies (e.g. Panessa et al. 2009; Bianchi et al. 2012). At present, some of the best unabsorbed Seyfert 2 candidates which have been quasi-simultaneously observed in the optical and X-rays are NGC 3147, NGC 3660 and Q 2131–427 (Bianchi et al. 2012).

From an observational point of view, unabsorbed Seyfert 2 [and Seyfert 2 without hidden BLR, (HBLR)] galaxies are predominantly found at low Bolometric luminosity or, correspondingly, low Eddington ratio (Bian & Gu 2007; Panessa et al. 2009; Shi et al. 2010; Wu et al. 2011; Marinucci et al. 2012). This is generally interpreted via theoretical models in which the broad-line region (BLR) is part of an outflow (e.g. Emmering, Blandford & Shlosman 1992; Murray et al. 1995; Nicastro 2000; Elitzur & Ho 2009; Trump et al. 2011). For instance, Nicastro (2000) proposes that the BLR originates in a disc-wind which is quenched below the critical mass accretion rate at which the accretion disc (AD) is gas-pressure-dominated throughout ($\dot{m}_{\rm crit} \sim 2.4 \times 10^{-3}$ in Eddington units and for typical radiative efficiency $\eta = 0.06$, viscosity parameter $\alpha = 0.1$, and black hole mass of $10^8\,{\rm M}_{\odot}$). Although unobscured/non-HBLR Seyfert 2 are indeed observationally confirmed to have accretion rates lower than the critical one (Trump et al. 2011; Bianchi et al. 2012; Marinucci et al. 2012), the mere existence of many type 1 Seyfert galaxies with clear BLR optical lines at much lower accretion rates represents a challenge for such model (e.g. M 81, Peimbert & Torres-Peimbert 1981; Filippenko & Sargent 1988; Ho 2008; Elitzur & Ho 2009). Indeed, the outflow model for the BLR/torus formation proposed by Elitzur & Ho (2009) on the basis of the original Elitzur & Shlosman (2006) description, predicts that the BLR should cease to exist only below $\dot{m}_{\rm crit} \sim 1 - 2 \times 10^{-6}$ (for a $10^8\,{\rm M}_{\odot}$ black hole), more than three orders of magnitude smaller than that proposed by Nicastro (2000).

Wang & Zhang (2007) have tested the Unified Model on a large sample of 243 local Seyfert galaxies and have proposed a scenario in which evolution plays an important role by controlling relevant physical parameters such as black hole mass and accretion rate, obscuring torus opening angle, and gas-to-dust ratio of the torus itself. Their evolutionary sequence for Seyfert galaxies starts with optically selected narrow-line-Seyfert 1 galaxies associated with high Eddington ratios and relatively small black hole masses, and ends with unabsorbed Seyfert 2 galaxies with no HBLR, a stage that is reached when the mass accretion rate is so low that the BLR disappears.

On the other hand, Wang et al. (2012) propose a different evolutionary sequence based upon the effects of star formation in AGN self-gravitating discs. These authors propose that warm skins are formed above a star-forming disc due to the diffusion of gas driven by supernova explosions, and show that the system evolution implies the episodic appearance of BLR with different properties, according to the specific evolutionary stage. In particular, Wang et al. (2012) predict the existence of an initial phase (phase I in their model) which is characterized by relatively high Eddington ratio and no BLR, as the line-emitting-region is still forming. These objects are predicted to be rare (and, for this reason, they are called Panda AGN) with a ∼1 per cent probability of occurrence in the overall population. Nevertheless, Panda AGN can in principle be distinguished from more typical low-luminosity unabsorbed Seyfert 2 galaxies because of their much higher Eddington ratio.

Here, we present results obtained from optical-to-X-ray observations of GSN 069, a soft X-ray variable, unabsorbed, high Eddington-ratio Seyfert 2 galaxy. We present quasi-simultaneous optical and X-ray spectra of this peculiar source, and we discuss our observational results in the context of models for the BLR in AGN, as well as their application to this particular case of a radiatively efficient unobscured Seyfert 2 galaxy candidate.

2 THE CASE OF GSN 069

A relatively bright ultrasoft X-ray source was detected on 2010–07–14 during an *XMM–Newton* slew from a position consistent with the galaxy GSN 069 (a.k.a. 6dfg 0119087–341131) at redshift $z = 0.0181$. *XMM–Newton* recorded an EPIC–pn count-rate of ∼1.5 counts^{-1}s in the soft 0.2–2 keV band, corresponding to a flux of $\sim 2.4 \times 10^{-12}$ erg s^{-1} cm^{-2}, according to the best available spectral decomposition (see sections below). Previous *ROSAT* pointed observations performed ∼16 yr earlier failed to detect the source, from which we infer that GSN 069 was at least 240 times fainter in the soft X-rays than during the *XMM–Newton* slew detection. The source was subsequently monitored with *SWIFT* for about one year. In order to better characterize the X-ray spectrum and the short-time-scale variability of the source, we obtained a further ∼15 ks *XMM–Newton* observation on 2010–12–02 which again detected the source in the soft X-rays at a similar flux level (Saxton et al. 2011).

GSN 069 was also detected in the far and near UV with *Galaxy Evolution Explorer* (*GALEX)* and is present in the *Wide-field Infrared Survey Explorer* (*WISE)* all-sky data release as well as in the Two Micron All Sky Survey (2MASS) point-source catalogue. Fig. 1 shows a 4 arcmin × 4 arcmin region of the *WISE* three-colour image centred on GSN 069 together with the *XMM–Newton* EPIC-pn contours from the 2010 pointed observation. Two, consistent, optical spectra, taken in 2001 and 2003 in the 2dF and 6dF surveys of the Anglo–Australian Telescope (AAT) show unresolved Balmer lines with no apparent broad components which, together with the diagnostic line ratios, classify the source as a Seyfert 2 galaxy. Here we report results from our X-ray (*XMM–Newton* and *Swift*) observations of this peculiar Seyfert 2 galaxy as well as from a new AAT optical spectrum obtained ∼3.5 months after the *XMM–Newton* slew detection. We complement our work with archival data which enable us to build the IR-to-X-ray spectral energy distribution (SED) of the source.

Throughout the paper, we adopt a cosmology with $H_0 = 70$ km s^{-1} Mpc^{-1}, $\Omega_{\Lambda} = 0.73$ and $\Omega_{\rm M} = 0.27$.

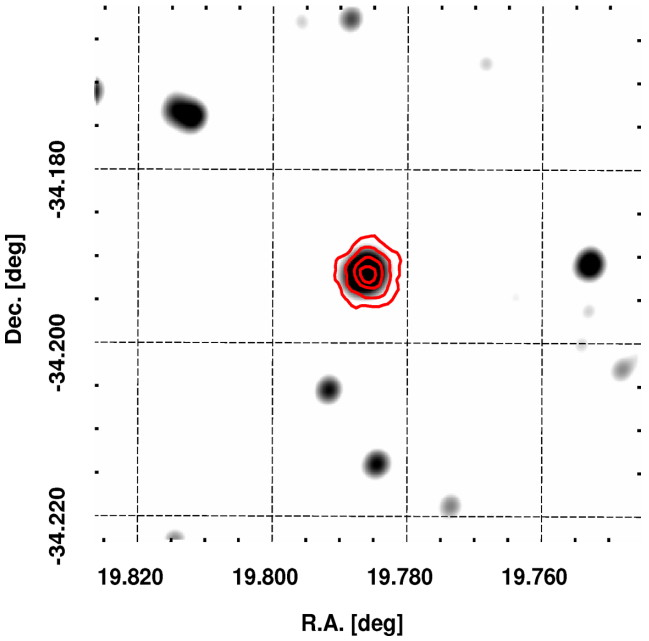

Figure 1. A 4 arcmin × 4 arcmin *WISE* three-colour image centred on GSN 069. The contours are from the *XMM–Newton* pointed observation. The UVOT-enhanced *Swift* X-ray position is RA: $01^{h}19^{m}08\overset{s}{.}66$ and Dec.: $-34^{\circ}11'30''4$ with a 90 per cent error of 1.9 arcsec in radius. The *Swift* error-circle lies within the innermost *XMM–Newton* contour.

3 OBSERVATIONS

The *XMM–Newton* slew (9194000004), which detected GSN 069 for the first time on 2010–07–14 with a soft X-rays count rate of 1.5 ± 0.4 counts s^{-1}, was performed with the EPIC-pn camera operated in full frame mode with the medium optical filter applied. GSN 069 was then the target of a pointed *XMM–Newton* observation on 2010-12-02 performed in full frame mode with the thin optical filter applied. The data were reduced as standard using the dedicated SAS v11.0 software. The final net exposures are ∼11 ks in the pn and ∼14 ks in the two MOS cameras. The EPIC pn, MOS 1 and MOS 2 spectra were grouped using the `specgroup` SAS task so that (i) each group has a signal-to-noise ratio S/N ≥ 4, and (ii) no group oversamples the full width at half-maximum (FWHM) instrumental resolution at the central energy of the group by more than a factor of 3. All groups comprise more than 20 background-subtracted counts, enabling us to use the χ^2 statistic for spectral fitting. The estimated background counts are comparable to the source-only ones above ∼0.95 keV in the pn spectrum, and above ∼0.7 keV in the MOS 1 and 2. We then consider here the X-ray data above 0.3 keV and below the above detector-dependent high-energy threshold. The RGS data were also reduced, but the short exposure and relatively low flux in the soft X-rays make them effectively meaningless for spectral analysis. During the observation, simultaneous optical and UV data were collected with the Optical Monitor (OM) with filters *B* (∼4500 Å), *W*1 (∼2900 Å) and *M*2 (∼2300 Å).

GSN 069 was monitored with 13 *Swift* observations performed in standard pc mode from 2010–08–26 to 2011–08–18. The data were reduced as standard. As none of the individual *Swift*-XRT spectra is of high enough quality to perform detailed spectral analysis, the XRT data are used here to construct the 0.5–2 keV flux light curve of GSN 069 during the ∼1 yr monitoring of the source. The X-ray data were complemented with photometry from the Ultraviolet/Optical Telescope (UVOT) which was operated in the *U* and/or *W*1 filters. *U* and *W*1 magnitudes of the source were 16.7 in both filters with no significant variation, in agreement with the *XMM–Newton* OM photometry.

We observed GSN 069 with the AAOmega 2dF spectrograph (Saunders et al. 2004; Sharp et al. 2006) at the focus of the AAT on 2010–10–27 for 3 × 600 s. We used the 580V (3700–5800 Å) and 385R (5600–8800 Å) low-resolution gratings ($R \sim 1300$). The 2dF data were reduced using the 2DFDR software of the AAT (e.g. Sharp & Birchall 2010) which performs bias subtraction, fibre-flat fielding and wavelength calibration in an automated manner. The response curves for the blue and red arms were determined with an observation of the bright DA white dwarf EG21 and were then used to obtain a relative flux calibration of the spectrum of GSN 069. The spectrum was then re-normalized to the *B*-band (∼4500 Å) *XMM–Newton* flux.

4 THE X-RAY VARIABILITY OF GSN 069

All available X-ray observation dates and soft X-ray fluxes are reported in Table 1. The historical X-ray light curve of GSN 069 is shown in Fig. 2, in terms of observed X-ray flux in the 0.2–2 keV band. The *ROSAT* data are not shown for clarity. However, as reported in Table 1, the source was not detected during the *ROSAT* All-Sky-Survey (RASS) and was also undetected in pointed Position Sensitive Proportional Counter (PSPC) observations in 1993 July and 1994 June. The most stringent 2σ upper limit comes from the PSPC observation on 1994-06-29 which can be used to obtain a

Table 1. GSN 069 observation dates and 0.2–2 keV fluxes. The fluxes have been estimated assuming a simple blackbody model and Galactic absorption fit to the pointed *XMM–Newton* observation. As the spectral model is simpler than the best-fitting one (also comprising significant warm absorption, see Section 5), the observed flux during the *XMM–Newton* pointed observation is about 10 per cent higher than that reported here. We however prefer to use the simpler spectral model here to ease comparison with future observations. Quoted uncertainties are given at the 2σ confidence level and are statistical only, while systematic, model-dependent uncertainties may be larger.

Mission	Date	Flux[a]
RASS	1990	<0.05
ROSAT-PSPC	1993-07-13	<0.009
ROSAT-PSPC	1994-06-29	<0.007
XMM slew	2010-07-14	2.4 ± 0.7
SWIFT	2010-08-26	2.1 ± 0.6
SWIFT	2010-08-27	2.1 ± 0.3
SWIFT	2010-10-27	1.8 ± 0.3
SWIFT	2010-11-24	1.6 ± 0.3
XMM pointed	2010-12-02	2.03 ± 0.03
SWIFT	2010-12-22	1.4 ± 0.3
SWIFT	2011-01-19	1.4 ± 0.3
SWIFT	2011-02-16	1.5 ± 0.3
SWIFT	2011-04-25	1.4 ± 0.3
SWIFT	2011-05-23	1.7 ± 0.3
SWIFT	2011-06-20	1.8 ± 0.3
SWIFT	2011-07-17	1.4 ± 0.3
SWIFT	2011-08-15	2.0 ± 0.3
SWIFT	2011-08-18	1.9 ± 0.5

[a]Flux in the 0.2–2 keV band in units of 10^{-12} erg s^{-1} cm^{-2}.

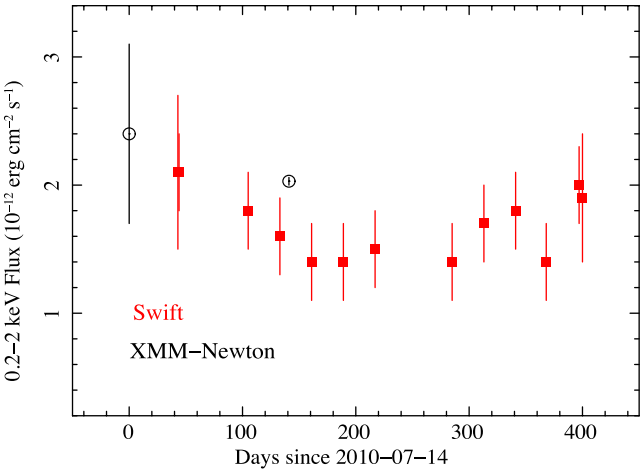

Figure 2. Historical 0.2–2 keV observed flux of GSN 069 since the *XMM–Newton* slew detection on 2010-07-14. Open circles represent the *XMM–Newton* pn slew and pointed observations; filled boxes are from the *Swift*-XRT detector (see Table 1).

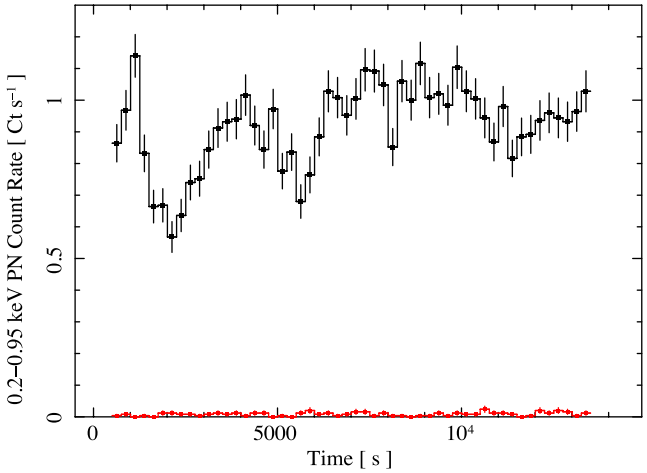

Figure 3. The soft (0.2–0.95 keV) X-ray EPIC-pn light curve of GSN 069 from the *XMM–Newton* pointed observation. The background light curve is also shown for reference after being corrected for the extraction area. We use a bin size of 250 s for both light curves.

0.2–2 keV flux of $\leq 7 \times 10^{-15}$ erg s^{-1} cm^{-2}, a factor of $\geq$240 lower than the observed flux during the *XMM–Newton* slew ∼16 yr later, and a factor of $\geq$280 lower than during the pointed observation on 2010-12-02. During the ∼1 yr-long monitoring which followed the *XMM–Newton* slew detection, the soft X-ray flux of GSN 069 exhibits variability on all probed time-scales (down to a few hundreds of seconds, see below), but was stable to within a factor of 2 during the monitoring campaign (see Fig. 2). This allows us to exclude that the X-ray activity is associated with a fast, transient phenomenon such as a tidal disruption event for which a fast decline of the X-ray emission is observed (e.g. Esquej et al. 2008; Saxton et al. 2012).

4.1 Short–time-scale X-ray variability and black hole mass estimates

The *XMM–Newton* pointed observation is long enough (∼15 ks) to investigate the short–time-scale variability of the source. The EPIC-pn light curve of GSN 069 in the soft (0.2–0.95 keV) X-ray band is shown in Fig. 3. Significant variability is detected down to the bin size (250 s). Since the excess variance $\sigma^2_{\rm rms}$ is anticorrelated with the black hole mass (e.g. Nikolajuk, Papadakis & Czerny 2004), X-ray variability can be used to obtain an estimate of the black hole mass in GSN 069. We refer to Ponti et al. (2012) for the operative definition of $\sigma^2_{\rm rms}$ and its error. We compute $\sigma^2_{\rm rms}$ from the 0.2–0.95 keV light curve shown in Fig. 3 using an interval of 10 ks duration and a bin size of 250 s. This choice corresponds to the $\sigma^2_{\rm rms,10}$ of Ponti et al. (2012) and we measure $\sigma^2_{\rm rms,10} = 3.4^{+6.6}_{-0.5} \times 10^{-2}$. As shown by Ponti et al. (2012), the excess variances in the soft and hard X-ray bands obey a tight 1:1 correlation. Hence, we can use the derived $\sigma^2_{\rm rms,10}$ in the soft band to obtain an X-ray-variability estimate of the black hole mass in GSN 069 by using the correlations of fig. 3 in Ponti et al. (2012), which were originally derived from the 2–10 keV light curves. Considering the scatter in their Fig. 3 rather than the errors on their best-fitting relation, we infer a black hole mass in the range $M_{\rm BH,\,X} \sim 0.3 - 7 \times 10^6$ M$_\odot$ in GSN 069.

An independent estimate of $M_{\rm BH}$ can be obtained from its relationship with the bulge *K*-band luminosity (Marconi & Hunt 2003). For typical seeing conditions during 2MASS observations and typical bulge sizes of 0.5–1 kpc, galaxy bulges are likely unresolved beyond redshift $z \sim 0.01$. Hence, we consider the point-source 2MASS catalogue which gives $m_{\rm K} = 13.89$ ($M_{\rm K} = -20.6$). Assuming negligible AGN contribution (see also Section 7), this translates into $M_{\rm BH,\,K} \lesssim 5 \times 10^6$ M$_\odot$, in good agreement with $M_{\rm BH,\,X}$. A further estimate may be derived from the $M_{\rm BH}-\sigma_*$ relationship assuming that the narrow-line-region (NLR) emitting gas traces the stellar gravitational potential of the bulge (i.e. assuming $\sigma_{\rm gas} = \sigma_\star$). The relatively low resolution of our optical spectrum only gives $\sigma_{\rm [O\,III]} \leq 120$ km s^{-1}, which translates into an upper limit of $M_{\rm BH,\sigma_{gas}} \leq 8.7 \times 10^6$ M$_\odot$, also consistent with the other estimates (we use the $M_{\rm BH}-\sigma_*$ relation resulting from the fits of the full sample of Xiao et al. 2011). We conclude that all available estimates of $M_{\rm BH}$ consistently indicate that $M_{\rm BH} \simeq 10^6$ M$_\odot$, although with relatively large uncertainties. As we show below, a consistent estimate is also obtained from our UV-to–X-ray spectral modelling.

5 THE X-RAY SPECTRUM OF GSN 069

The only X-ray observation with sufficient quality for detailed spectral analysis is the pointed *XMM–Newton* observation performed on 2010-12-02. The X-ray spectrum that can be obtained by merging all *Swift*-XRT observations contains ∼13 times less X-ray counts than that from the pointed *XMM–Newton* observation. We then only discuss here the spectral analysis from the latter data set. Since fits to the individual pn and MOS spectra gave consistent results, all instruments were fitted simultaneously, compensating any residual normalization difference between the EPIC cameras with a constant. A simple power-law model and Galactic absorption (with $N_{\rm H} \equiv 2.48 \times 10^{20}$ cm^{-2}, Kalberla et al. 2005) cannot reproduce the data [$\chi^2 = 516$ for 29 degrees of freedom (d.o.f.)] and yields a very steep, unphysical photon index ($\Gamma \simeq 6.7$).

We then replace the power law with a phenomenological (redshifted) blackbody model in the attempt to describe the very soft spectrum. The X-ray data are now reasonably well reproduced ($\chi^2 = 47$ for 29 d.o.f.) with a blackbody temperature of 58 ± 2 eV. However, clear residuals in the form of a likely absorption structure are left around 0.7 keV. In the upper panel of Fig. 4, we show the data, model and residuals, showing the 0.7 keV absorption structure seen in the data. We only show the EPIC-pn data, although the MOS ones are also included in the fit. Adding a phenomenological edge

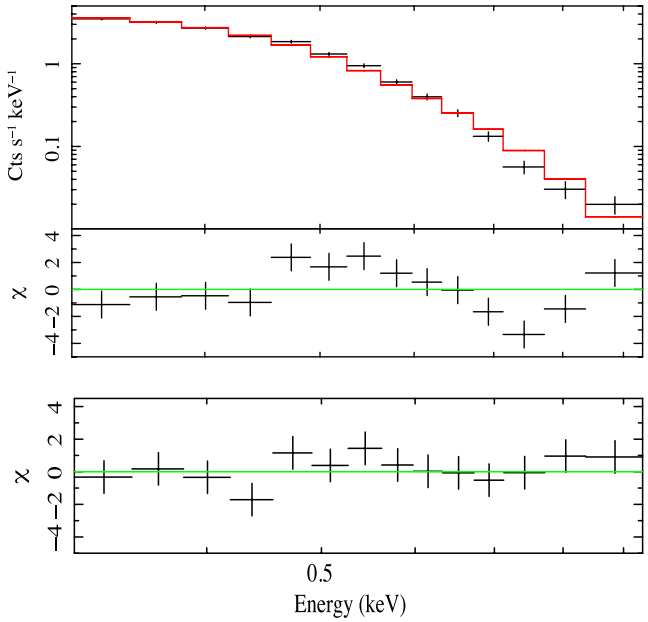

Figure 4. Upper: the EPIC pn (black) spectrum, model and residuals (in terms of σ) for a simple blackbody model and Galactic absorption. An extra absorption feature is present around 0.7 keV indicating the presence of ionized gas in the LOS. Lower: best-fitting residuals obtained by adding a warm absorber with $N_{\rm H} \sim 1 \times 10^{22}$ cm^{-2} and $\log \xi \sim 0.40$.

model with (rest-frame) energy $E_{\rm edge} \simeq 0.67$ keV and optical depth $\tau \simeq 0.8$ provides a significant improvement of the fitting statistic ($\chi^2 = 25$ for 27 d.o.f.), showing that an absorption feature is a viable explanation of the residuals in the data, most likely indicating the presence of partially ionized gas in the LOS. We then replace the edge with a more self-consistent warm absorber model, namely the ZXIPCF model (Reeves et al. 2008), and obtain a good description of the data ($\chi^2 = 24$ for 27 d.o.f.) for an ionized absorber with column density $N_{\rm H} = 1.0^{+0.6}_{-0.7} \times 10^{22}$ cm^{-2} and ionization parameter $\log \xi = 0.40^{+0.09}_{-0.07}$. The blackbody temperature is now 60 ± 2 eV. No statistical improvement is obtained by adding a further neutral absorption intrinsic component (i.e. at redshift $z = 0.018$) with $N_{\rm H}^{z} \leq 2 \times 10^{20}$ cm $^{-2}$. The residuals for our final best-fitting model are shown in the lower panel of Fig. 4.

Our phenomenological blackbody model provides a fair description of the X-ray *XMM–Newton* spectrum of GSN 069, once warm absorption is taken into account. The inferred temperature of $kT \sim 60$ eV is significantly cooler than that of the typical soft X-ray excess in AGN which, when described in terms of thermal emission, is generally in the range of 100–200 eV (e.g. Piconcelli et al. 2005; Crummy et al. 2006; Miniutti et al. 2009). The temperature derived for GSN 069 is in fact consistent with that expected from thermal AD emission for a relatively small-mass black hole radiating close to its Eddington limit, so that the most natural interpretation for the spectral shape is that it represents the high-energy tail of the disc emission.

On the other hand, other spectral models can equally well describe the data. In particular, the soft X-ray spectrum of GSN 069 may result from strong Comptonization of a seed photons spectrum in a corona with plasma temperature $kT_{\rm e}$ and optical depth $\tau_{\rm e}$. However, Comptonization models suffer from a well-known series of parameter degeneracies when applied to limited bandpass data. In particular, the observed spectrum can be well reproduced by assuming a low seed photons temperature ($\sim$10 eV) and a corona with $kT_{\rm e} \sim 60$ eV and large optical depth ($\tau_{\rm e} \gtrsim 10$). However, the same spectral shape can also be obtained by increasing the seed photons temperature as well as $kT_{\rm e}$, and by lowering $\tau_{\rm e}$ in order not to overproduce high-energy X-rays. In summary, the properties of the putative X-ray corona are largely unconstrained by our data. Hence, although we caution that the spectrum may well be interpreted in terms of Comptonized emission, we refrain from applying Comptonization models to the X-ray data here.

5.1 A more physical description

The best-fitting blackbody model described above underpredicts the simultaneous UV data from the OM by more than two orders of magnitude.[1] Although the OM fluxes are likely contaminated by the host galaxy emission, it seems unlikely that the AGN does not contribute at all at least at the shortest wavelengths. The flux in the shortest-wavelength M2 filter at $\sim$2300 Å is underpredicted by a factor of $\sim$250 by the best-fitting X-ray model.

We then replace the blackbody with a more physical AD model, namely the OPTXAGNF model (Done et al. 2012; Jin et al. 2012) and consider simultaneous fits to the X-ray and UV (M2-filter only) data. The main model assumptions are the following: the disc emits a colour-corrected blackbody down to a given coronal radius $r_{\rm c}$, and the corona is assumed to comprise a two-phase plasma. Within the corona, the available energy is distributed between powering the soft X-ray excess via Comptonization in an optically thick plasma, and the standard high-energy power law via Comptonization in an optically thin phase.

We first assume a pure thermal AD model, with no additional Comptonization component(s). The model depends on black hole mass, Eddington ratio and black hole spin. We found that statistically equivalent fits could be obtained with non-spinning and maximally spinning black hole models. For the case of a non-rotating Schwarzschild black hole, the model provides a fair description of the UV and X-ray data with a reduced χ^2/d.o.f. = 25/28. The best-fitting model implies a black hole mass of $M_{\rm BH} = (1.2 \pm 0.1) \times 10^6$ M$_\odot$ and $L_{\rm Bol}/L_{\rm Edd} = 0.51 \pm 0.05$. The warm absorber properties are $N_{\rm H} = (8.6 \pm 1.2) \times 10^{21}$ cm^{-2} and $\log \xi = 0.35 \pm 0.07$, consistent with those derived with the simpler model discussed above. If a maximally rotating Kerr black hole is assumed instead, the data are reproduced with the same statistical quality but with larger black hole mass ($M_{\rm BH} \sim 8.5 \times 10^6$ M$_\odot$) and lower Eddington ratio ($\sim$0.06). We conclude that a thermal AD plus X-ray warm absorption model provides a reasonable description of the X-ray and shortest-wavelength UV data of GSN 069.

Next, we consider the possible presence of Comptonization in the framework of the OPTXAGNF model. As no high-energy power law is seen in the data, we assume that all the energy available to the corona powers only the soft excess emission, which depends on the seed photons temperature (self-consistently derived from black hole mass and Eddington ratio) and on the coronal parameters ($kT_{\rm e}$ and $\tau_{\rm e}$) and size ($r_{\rm c}$). However, the UV data from the *M*2 filter are not sufficient to remove the degeneracies of the Comptonization model, and we cannot constrain all the parameters independently. We only report here results from one particular case, chosen because

[1] In extrapolating the best-fitting X-ray model, we consider UV reddening by assuming the standard gas-to-dust conversion $E(B-V) = 1.7 \times 10^{-22}$ $N_{\rm H}$ for the Galactic column density using the UVRED model (valid between 1000 and 3704 Å): Furthermore, we assume that the X-ray warm absorber is dust-free, so does not contributes in the UV.

such configuration is often invoked as an explanation for the soft X-ray excess in AGN (e.g. Done et al. 2012; Jin et al. 2012). We assume that the corona is strongly optically thick with $\tau_e = 13$, corresponding to the average value for the coronal optical depth in the study of a relatively large sample of type 1 AGN by Jin et al. (2012) who used the same spectral model (OPTXAGNF). The fit is statistically good (χ^2/d.o.f. = 24/27), and we obtain $kT_e = 70 \pm 20$ eV for a black hole mass of $M_{BH} = (0.9 \pm 0.1) \times 10^6\,M_\odot$ and $L_{Bol}/L_{Edd} = 0.94 \pm 0.06$, corresponding to a Bolometric luminosity of $0.9 - 1.3 \times 10^{44}$ erg s^{-1}.

As Comptonization is consistent but not required by the data, and given that the coronal physical parameters cannot be constrained independently, we consider that the pure AD model is the simplest best-fitting description of the UV-to–X-ray spectrum of GSN 069, with the caveat that we cannot exclude that the soft X-ray emission is in fact Comptonized. The observed 0.5–2 keV flux is $\sim 1.8 \times 10^{-13}$ erg s^{-1} cm^{-2} yielding an unabsorbed luminosity of $\sim 1.2 \times 10^{42}$ erg s^{-1} in the same band (we extrapolate our best-fitting up to 2 keV, and we refer to the commonly used 0.5–2 keV band to ease the comparison with other sources and observatories). On the other hand, the 2–10 keV luminosity is $\leq 4.4 \times 10^{40}$ erg s^{-1}. The overall Bolometric luminosity is $\sim 8 \times 10^{43}$ erg s^{-1}, corresponding to an Eddington ratio of $\sim$0.5 and a black hole mass of $\sim 1.2 \times 10^6\,M_\odot$ for a non-rotating black hole.

6 OPTICAL PROPERTIES: GSN 069 AS A TRUE SEYFERT 2 GALAXY CANDIDATE

Two consistent 2dF and 6dF optical spectra taken in 2001 and 2003 at the AAT show unresolved Balmer lines with no apparent broad components. The standard diagnostics emission line ratios [O III]λ5007/Hβ $\sim$ 9.2 and [N II]λ6583/Hα $\sim$ 1.4 from the 2001/2003 spectra classify GSN 069 as a Seyfert galaxy, well separated from low-ionization nuclear emission-line regions (LINERs) and composite/star-forming galaxies (Baldwin, Phillips & Terlevich 1981; Veilleux & Osterbrock 1987; Ho, Filippenko & Sargent 1997). The lack of broad components indicates that GSN 069 appears to be a rather typical Seyfert 2 galaxy in the optical at epoch 2001/2003. The dramatic X-ray brightening of the source between 1994 and 2010 prompted us to perform a new optical spectroscopic observation with the goal of investigating any variability of the optical spectrum and, in particular, to search for the appearance of any broad-line component. A new optical spectrum was then taken at the AAT on 2010-10-27, $\sim$3.5 months after the *XMM–Newton* slew detection.

The spectrum has been fitted to a linear combination of spectral templates of evolutionary star formation episodes from Bruzual & Charlot (2003) plus a power law to account for any AGN continuum. We point out that replacing the arbitrary power law in the optical range with our UV-to–X-ray best-fitting pure AD model (Section 4.1) works very well and gives the same results. The remaining emission lines have been fitted with Gaussian profiles in the residuals of the stellar template fit. All can be fitted with narrow Gaussian components, and we do not detect any broad component in any of the emission lines down to the instrumental resolution, as was the case also in the earlier 2001/2003 2dF and 6dF spectra. The diagnostic line ratios are unchanged with respect to previous measurements, as expected given the typical geometrical scale of the NLR, namely hundreds-thousands of light years.

The optical properties of GSN 069 classify it as a Seyfert galaxy whose optical BLR is either obscured, absent or gives rise to undetectable broad emission lines. The lack of X-ray cold absorption and, perhaps most importantly, the fast X-ray variability at soft X-ray energies, rules out a standard Seyfert 2 galaxy interpretation, so that it appears unlikely that the BLR of GSN 069 is obscured. The remaining possibilities are that (i) the BLR is present, but we are unable to detect the corresponding broad lines in the available optical spectra or (ii) GSN 069 is a true Seyfert 2 galaxy lacking the BLR.

It is instructive, at first, to estimate the FWHM and luminosity of the broad lines that we may expect to be present in GSN 069. We focus here on the Hα emission line, as it is significantly stronger than Hβ. From our best-fitting spectral model, we can extract estimates of the black hole mass and intrinsic continuum monochromatic luminosity at 5100 Å. By using the standard, reverberation-mapping-calibrated relationship (e.g. Xiao et al. 2011) between optical luminosity, line FWHM, and black hole mass, we infer that GSN 069 should exhibit broad lines with FWHM$\sim$1300 km s^{-1}, which would classify it as a typical NLS1 galaxy. On the other hand, by using the empirical relation between broad Hα and continuum luminosities from Greene & Ho (2005) as updated in Xiao et al. (2011), we estimate $L^{est}_{H_\alpha} \sim 3.7 \times 10^{40}$ erg s^{-1} for the broad component in GSN 069.

The new 2010 AAT optical spectrum is shown in Fig. 5 around the Hβ–[O III] and around the Hα–[N II] regions. We superimpose on the observed Hα spectrum the expected broad Hα component, assuming the FWHM and broad $L^{est}_{H_\alpha}$ estimated above. It is quite clear that, were the broad Hα line present, we would have securely detected it, unless its properties (FWHM and luminosity) were very peculiar. We must conclude that GSN 069 either lacks the BLR or that the corresponding emission lines are unusually weak. In the first case, GSN 069 appears to be a bona-fide true Seyfert 2 galaxy candidate (although spectropolarimetric observations would be needed to exclude the presence of HBLR).

7 BROAD-BAND SED

We have collected all photometric information available for GSN 069 from various catalogues. Multi-epoch data exist in the optical B_j and R bands. No significant variability is present and $B_j \simeq 16.2$ and $R \simeq 15.3$ over $\sim$30 yr time-scales.[2] On the other hand, some variability in the UV is present, as the *GALEX* 2007 flux appears to be $\sim$50 per cent higher than that from the 2010 *XMM–Newton* OM observation.

The Galactic-absorption-corrected SED of GSN 069 is shown in Fig. 6 together with a plausible model. The longest wavelength *WISE* data are accounted for by a Starburst template obtained from 16 Starburst galaxies with redshift $\leq$1.3 observed with *Spitzer*/IRS (Hernán-Caballero & Hatziminaoglou 2011). The 2MASS and optical data are dominated by a combination of spectral templates of evolutionary star formation episodes with ages between 900 Myr and 5 Gyr (Bruzual & Charlot 2003), plus a $\sim$10 per cent AGN contribution. The UV-to–X-ray data are well reproduced by the pure AD SED, modified by absorption from dust-free partially ionized

[2] GSN 069 is present in the USNO–B1.0 and USNO–A2.0 catalogues where magnitudes $B_j \sim 12-13$ and $R \sim 12$ are reported for epochs $\leq$1998. However, we have analysed the corresponding digitized plates in the B_j and R bands and we have compared GSN 069 count rate with those from two reference stars in all plates and in the *XMM–Newton* B-band OM observation. We do not confirm the magnitudes reported in those catalogues and we infer a maximum 60 per cent variability in the B_j band between 1980 and 2010. Our analysis is also supported by the reported $B_j = 16.03$ obtained during the Durham/SAAO survey at epoch $\sim$1983.4 by Metcalfe et al. (1989).

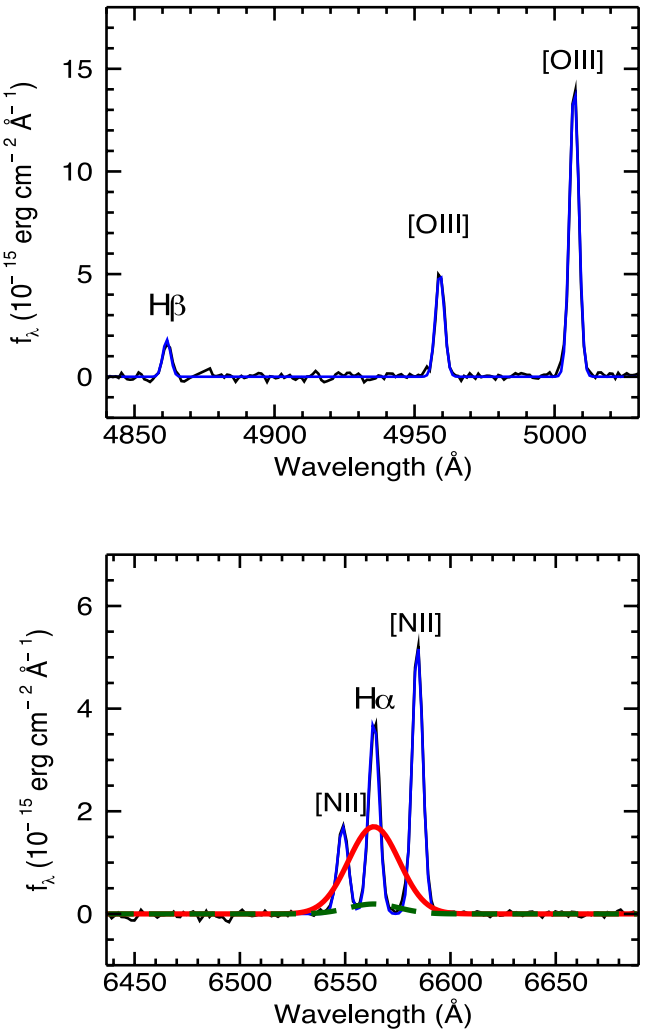

Figure 5. The optical residual spectrum of GSN 069 from the 2010–10–27 AAT observation in the Hβ and [O III] (upper panel) and Hα and [N II] region (lower panel) after subtracting the stellar contribution is shown in black. All emission lines have been fitted with unresolved Gaussian lines (blue solid line). We also show as a dotted–dashed line the expected broad Hα component (see the text for details). The green line is a broad Gaussian with the same FWHM and with intensity ∼3 times the residuals, i.e. a representation of the broad component upper limit. Its luminosity is ∼9 times lower than that we would expect to be present in GSN 069.

gas in the X-rays (and unobservable EUV range) which provides a good fit in the UV-to–X-ray band (Section 4.1). The discrepancy between the UV *XMM–Newton* OM and *GALEX* data (2010 and 2007 respectively) falls into the AGN-dominated spectral region, so that it can be naturally explained by moderate AGN variability. The gentle rise towards shorter wavelengths of the *GALEX* data points confirms the general AGN intrinsic spectral shape in that region.

8 DISCUSSION I: X-RAY PROPERTIES AND COMPARISON WITH SIMILAR SOURCES

We present our discussion of the observational results in two steps. Here, we discuss the extreme long-term X-ray variability of GSN 069 and the lack of hard X-ray emission, and we compare its most peculiar properties with a similar, newly discovered AGN as well as with the class of black hole binaries. We also discuss how GSN 069-like sources (with more typical, larger black hole mass) may be missed and misclassified in current X-ray surveys. A detailed discussion on the lack of BLR lines is deferred instead to Section 9.

The present (2010) Bolometric luminosity of GSN 069 is ∼8 × 10^{43} erg s^{-1}, corresponding to an Eddington ratio $\lambda \simeq 0.5$ for a 1.2 × 10^6 M$_\odot$ black hole. The luminosity was likely similar or slightly higher in 2007, as suggested by the *GALEX* fluxes (Fig. 6). An estimate of the past Bolometric luminosity of GSN 069 can be obtained by applying Bolometric corrections to the NLR emission lines. As the NLR are likely located hundreds to thousands of light years away from the nucleus, the NLR-based luminosity represents an estimate of the average Bolometric luminosity that GSN 069 had in the past. Hereafter, we refer to that estimate as the *historical* Bolometric luminosity of the source. $L_{\rm Bol}^{\rm hist}$ can be estimated from the extinction-corrected Hα and/or [O III] luminosity. We obtain $L_{\rm Bol}^{\rm hist} \sim 3.1 \times 10^{42}$ erg s^{-1} from the Hα luminosity with the Greene & Ho (2005) Bolometric correction, and a consistent $L_{\rm Bol}^{\rm hist} \sim 2.3\text{-}5.2 \times 10^{42}$ erg s^{-1} by applying the luminosity-dependent Bolometric corrections of Lamastra et al. (2009) or Stern & Laor (2012) to the [O III] luminosity. Hereafter we assume $L_{\rm Bol}^{\rm hist} \sim 3.1 \times 10^{42}$ erg s^{-1}, corresponding to an Eddington ratio $\lambda^{\rm hist} \sim 2 \times 10^{-2}$ for a black hole mass of $M_{\rm BH} \sim 1.2 \times 10^6$ M$_\odot$. We conclude that GSN 069 is much more luminous now than in the past with a Bolometric luminosity ∼20–30 times higher than the historical one.

8.1 Extreme long-term X-ray variability

The comparison between the *XMM–Newton* and *Swift* observations and the *ROSAT* non-detection of the source implies that GSN 069 was at least a factor of ≥280 fainter in the soft X-rays in 1994 than it is now. As our best-fitting spectral model for the *XMM–Newton* pointed observation comprises significant absorption from partially ionized gas, one possibility is that changes in the absorber's properties are responsible for the dramatic X-ray flux variation. For instance, the flux variability can be fully accounted for by assuming that the absorber's column density was ≥8.2 × 10^{22} cm^{-2} during the *ROSAT* observation.

Another possibility is, however, more appealing to us. As discussed above $L_{\rm Bol}^{\rm hist} \sim 3.1 \times 10^{42}$ erg s^{-1} was 20–30 times lower than the present $L_{\rm Bol}$. If the gas responsible for the X-ray warm absorber has the same properties (density and distance) in both past low-luminosity and present high-luminosity states, its ionization state would have been lower by a similar factor in the past, which further depresses the soft X-rays due to increased opacity. Indeed, if the Bolometric luminosity and warm absorber ionization are both lowered by a factor of ≥15, the expected soft X-ray flux is lower than the *ROSAT* upper limit, thus providing a clean, self-consistent explanation for the non-detection by *ROSAT*. In summary, the extreme X-ray brightening by a factor of ≥280 from 1994 to 2010 can be explained by a much more reasonable factor of ≥15 in luminosity, consistent also with the comparison between the historical and present Bolometric luminosity estimates.

8.2 On the lack of hard X-rays in GSN 069

The intrinsic 0.5–2 keV luminosity of GSN 069 is $L_{0.5\text{–}2} \simeq 1.2 \times 10^{42}$ erg s^{-1}, while the 2–10 keV luminosity is $L_{2\text{–}10} \leq 4.4 \times 10^{40}$ erg s^{-1}. As shown e.g. in Miniutti et al. (2009) the 0.5–2 keV

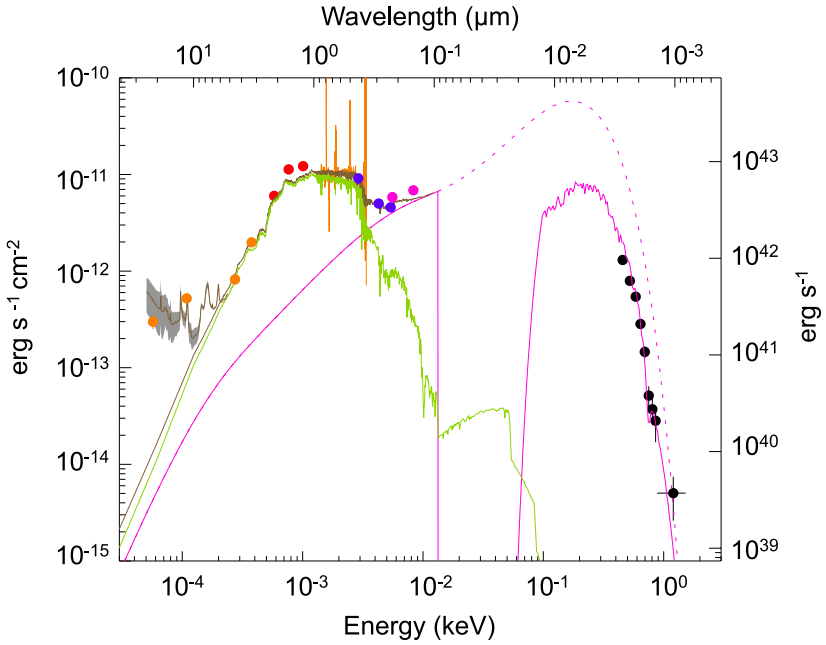

Figure 6. The Galactic-absorption-corrected SED of GSN 069 from 22 μm to 1.5 keV, see the text for details. From left to right we show data from *WISE* (orange), 2MASS (red), AAT (orange), *XMM–Newton* OM (blue), *GALEX* (pink) and *XMM–Newton* EPIC-pn (black). The AGN intrinsic SED is shown as a dotted line, while the effect of the X-ray dust-free warm absorber is shown as a solid line. The highest energy X-ray data point is not used in the spectral analysis due to the low significance of the detection above 0.95 keV, but is shown here as reference. The deep UV/EUV trough in the warm-absorbed SED is a simple estimate of the absorption due to neutral hydrogen of the warm absorber in that spectral range. No extinction is expected below 13.6 eV under the reasonable assumption that the warm X-ray-absorbing gas is dust-free.

and 2–10 keV luminosities obey a tight correlation in a sample comprising PG quasars and AGN with small black hole mass and high Eddington ratio (of the order of those estimated for GSN 069). According to that correlation (see their Fig. 4), the observed upper limit on L_{2-10} implies that the hard X-ray emission in GSN 069 is $\gtrsim$30 times fainter than in typical type 1 AGN, even considering AGN with similar black hole mass and Eddington ratio.

The upper limit on the 2–10 keV luminosity translates into a 2–10 keV X-ray Bolometric correction $k_{2-10} \geq 1800$. The typical k_{2-10}, as obtained e.g. in Vasudevan et al. (2009) does not exceed ∼100, i.e. it is more than one order of magnitude lower. GSN 069 can be classified as an (hard) X-ray weak AGN with an optical (2500 Å) to X-ray (2 keV) slope $\alpha_{ox} \leq -2.0$, while, based upon its intrinsic optical luminosity, we would expect $\alpha_{ox}^{expected} \sim -1.1$ (e.g. Just et al. 2007). In this sense, GSN 069 resembles the typical AGN in the sample of intermediate-mass black hole of Greene & Ho (2004, 2007), which is characterized by AGN with small black hole mass and relatively high Eddington ratio. In a recent work, Dong, Greene & Ho (2012) have shown that the α_{ox} values of their sample of AGN with black hole masses of 10^5–10^6 $M_\odot$ are systematically lower than the extrapolation of the well known α_{ox}–l_{2500} relationship derived from more massive systems, so that a significant fraction of AGN with low-mass black holes appear to be more X-ray weak than their massive counterparts. Some of these X-ray weak objects may be significantly absorbed, but absorption seems unable to explain the bulk of this population raising the possibility that some are intrinsically X-ray weak. As the Dong et al. (2012) sources are observationally biased towards high Eddington ratios, a connection between X-ray weakness and Eddington ratio seems plausible.

In this respect, GSN 069 may represent an extreme case of a high Eddington ratio system in which the standard (optically thin) X-ray corona is absent or unable to efficiently up-scatter the soft disc photons. Indeed, as shown in our spectral modelling, it is quite striking that the UV-to–X-ray data can be modelled with a pure AD spectrum with no X-ray corona at all. Among the possible explanations for the lack/weakness of optically thin coronal emission, we point out the work by Proga (2005) who discusses how a failed disc-wind may quench the coronal X-ray emission. In that situation, the relatively high density in the failed wind means that bremsstrahlung losses dominate over inverse Compton, thus quenching the hard X-ray emission, while preserving the soft X-rays.

8.3 Comparison with 2XMM J123103.2+110648

Terashima et al. (2012) and Ho, Kim & Terashima (2012) report the discovery and subsequent study of the AGN 2XMM J123103.2+110648, which shares many properties with GSN 069. The source is detected at soft X-ray energies only with similar 0.5–2 keV luminosity (∼2.5 × 10^{42} erg s^{-1}) to GSN 069. The X-ray spectrum of 2XMM J123103.2+110648 can be described by a pure AD model or by Comptonization in an optically thick plasma, as is the case for GSN 069.[3] 2XMM J123103.2+110648 is unabsorbed in the X-rays and does not show any broad Balmer lines in the optical, strongly suggesting that this AGN lacks the BLR too (or that the corresponding emission lines are much weaker than in typical AGN).

In summary, GSN 069 and 2XMM J123103.2+110648 are bona-fide true Seyfert 2 galaxies with relatively small black hole mass (10^5–10^6 $M_\odot$) and high Eddington ratio (∼0.5). Their soft X-ray emission is variable on both short and long time-scales, while no X-ray photons are securely detected above 1–2 keV. Besides the

[3] Based on X-ray flux and spectral variability Terashima et al. (2012) suggest that Comptonization is the most plausible interpretation.

lower temperature of the soft excess in GSN 069 (which may reflect a slightly higher black hole mass), the only apparent difference between the two sources is that GSN 069 appears to be more luminous now than in the past with $L_{\rm Bol}^{\rm present}/L_{\rm Bol}^{\rm hist} \sim 20-30$, while 2XMM J123103.2+110648 does not appear to have dramatically changed its radiative output, i.e. $L_{\rm Bol}^{\rm present}/L_{\rm Bol}^{\rm hist} \sim 1$–2 (Ho et al. 2012; Terashima et al. 2012).

8.4 GSN 069 in the wider context: X-ray binaries/AGN unification and Compton-thick AGN population

It is interesting to compare the peculiar SED of GSN 069 with that of black hole X-ray binaries. During their outbursts, these systems reach a so-called soft or thermal state that is dominated by thermal AD emission in the X-ray band. During the thermal state, a power-law component is generally seen, with a fractional contribution of $\lesssim$20 per cent (Remillard & McClintock 2006; Dunn et al. 2010). Some X-ray transients, however, do reach super-soft states in which the hard X-ray contribution appears to be negligible. Here we only mention the case of XTE J1650−500 which, during its 2001/2002 outburst, reached a super-soft state with a $\lesssim$0.5 per cent power-law contribution to the Bolometric luminosity (Motta et al. in preparation; private communication), as it is the case in GSN 069. The super-soft state in XTE J1650−500 lasted about one month which, accounting for a linear scaling between time-scales and black hole mass, would translate into the possibility that the super-soft state in GSN 069 may last as long as a few thousands of years. Considering that the overall outburst of XTE J1650−500 was about 6 months long, the duty cycle for such super-soft state may typically be of the order of 10–20 per cent in accreting black holes with Eddington ratios above few $\times\ 10^{-3}$. A study of the occurrence of these states in the known X-ray binary population will enable us to refine the above estimates.

On the other hand, variability properties define a striking difference between GSN 069 and black hole X-ray binaries in soft, thermal-dominated states. GSN 069 exhibits short–time-scale variability on time-scales as short as a few hundreds of seconds (Fig. 3), while the AD emission in black hole binaries is stable on time-scales $\lesssim$1 s (corresponding to $\lesssim 10^5$ s for a 10^6 M$_\odot$ black hole as in GSN 069). This may suggest that the soft X-ray in GSN 069 are Comptonized rather than purely thermal (as suggested by Terashima et al. 2012 for 2XMM J123103.2+110648) or that the AD structure in AGN is slightly different from that in X-ray binaries (maybe inhomogeneous and intrinsically more variable).

Finally, it is interesting to consider the observational analogy between GSN 069 and 2XMM J123103.2+110648 and heavily absorbed, Compton-thick type 2 AGN candidates. Both classes of sources are characterized by relatively strong narrow optical lines such as O III, the absence of broad optical lines, and the lack of detection in the hard X-rays (or, in any case, a high $L_{\rm O\,III}/L_{\rm X}$ ratio). The only difference between the two classes is that GSN 069 and 2XMM J123103.2+110648 are detected and variable (on short time-scales) in the soft X-rays, while the soft X-ray emission in Compton-thick AGN is related to reprocessing in large-scale photoionized plasma which is, by definition, weak and constant. If our interpretation of the soft X-ray emission in terms of AD thermal emission is valid, the detection of any soft X-ray emission in GSN 069 and 2XMM J123103.2+110648 is only possible thanks to their low black hole mass and relatively high accretion rate. More massive AGN with similar or smaller mass accretion rates have AD emission whose high-energy tail does not enter at all the soft X-ray band, so that large black hole mass analogues of GSN 069 will be missed in the X-rays. In fact, assuming a typical Eddington ratio $\lambda = 0.1$ and non-rotating black holes, the AD emission does not reach the soft X-ray band for $M_{\rm BH} \geq 10^7$ M$_\odot$ at low redshift, so that almost all GSN 069-like AGN would be misclassified as Compton-thick candidates in even moderately high-redshift surveys because of their relatively strong O III emission and lack of detection at X-ray energies.

Hence, there could be an entire population of AGN in super-soft states (in analogy with X-ray binaries) that are completely missed in current X-ray surveys. The time that AGN spend in super-soft states may be as long as 10^4–10^5 yr for typical black hole masses of 10^7–10^8 M$_\odot$ with a typical duty cycle of 10–20 per cent for Eddington ratios above few $\times\ 10^{-3}$, suggesting that the population of super-soft state AGN may be non-negligible. If so, GSN 069-like objects may contaminate the derived fraction of highly obscured AGN in the Universe because, as discussed above, they are likely counted as Compton-thick AGN in current X-ray surveys.

9 DISCUSSION II: ON THE LACK OF BROAD EMISSION LINES IN GSN 069

Although spectropolarimetric observations would be needed to conclude that GSN 069 and 2XMM J123103.2+110648 do not have HBLR, the lack of broad optical lines and of X-ray cold absorption, together with the observed short time-scale X-ray variability in the soft band, suggests that both AGN may have intrinsically very weak (or absent) BLR optical lines. Here we critically consider possible explanations for the lack of BLR in these objects in the framework of two popular BLR models.

9.1 Linking the lack of hard X-rays with the absence of the BLR

Both GSN 069 and 2XMM J123103.2+110648 are outstanding objects not only based on their optical and soft X-ray properties, but also because they lack hard X-ray emission, which has up to now been considered a hallmark property of accreting supermassive black holes. The lack of hard X-ray emission may be invoked to account naturally for the lack of broad optical emission lines if the BLR clouds need to be confined and in pressure equilibrium with a hot medium. Such two-phase BLR model was first proposed by Mathews (1974) and then refined by e.g. Wolfe (1974), McKee & Tarter (1975) and, in much more detail, by Krolik, McKee & Tarter (1981).

In particular, Krolik et al. (1981) show that, depending on the details of the radiation field, cold, dense gas (i.e. the BLR clouds) can coexist in pressure equilibrium with – and be confined by – hotter, less dense gas (typically with temperatures of $\sim 10^8$ K) at ionization stages consistent with that of the BLR. The state of the gas is determined by its thermal (and ionization) equilibrium with the irradiating radiation field. At the typical distances of the BLR, the temperature is roughly governed by the balance between Compton heating (by X-rays) and inverse-Compton cooling (see however Krolik et al. 1981, for a comprehensive study of other possible heating and cooling mechanisms). As clear, the predicted temperature sensitively depends on the hard X-ray flux which determines the amount of Compton-heating, without affecting so strongly the cooling which depends more on the overall spectrum. Krolik et al. (1981) show indeed that the extent of the multiphase region where cold BLR clouds are in pressure equilibrium with the hotter intercloud medium at the right ionization state is a monotonic function of the fraction of high energy photons in the radiation field. When hard X-rays are weak or even absent, the multiphase character of

the equilibrium solutions is lost, and cold, dense clouds cannot be confined by the hotter medium (see also Guilbert, McCray & Fabian 1983).

The two-phase model for the BLR thus predicts the disappearance of the BLR emission lines whenever the intercloud medium is not hot enough to support the colder/denser BLR clouds. As the Compton temperature tends towards the SED peak in νL_ν, one can visually estimate that it is roughly $\sim 10^6$ K in GSN 069 (see Fig. 6). Such temperature is nearly two orders of magnitude lower than that required to confine the cold line-emitting clouds in the BLR. It is then quite clear that the lack of hard X-rays in GSN 069 (and in 2XMM J123103.2+110648) corresponds to a case in which the Compton temperature is too low to sustain a multiphase medium, thus preventing thermodynamically the formation of a broad-line emitting region.

More examples of GSN 069-like objects with variable levels of hard X-ray emission would be crucial to confirm or discard this idea in the future (possible examples of hard X-ray emitters lacking the BLR may be Mrk 273x and 1ES 1927+654, as discussed by Bianchi et al. 2012). We will continue to monitor GSN 069 in the X-rays in the future. The detection of hard X-rays sometime in the future will prompt us to perform another optical/UV spectroscopic campaign on this peculiar object, which may be used to confirm/dismiss the above interpretation, and/or to assess the relevant heating/cooling time-scales associated with the two-phase BLR model observationally.

On the other hand, problems with the two-phase model discussed above have been subsequently recognized (see e.g. Mathews & Ferland 1987). In particular, the Compton temperature as derived from current detailed AGN SED is typically 10^7 K, too low from the BLR clouds to be stable against drag forces, or for the hot phase to be optically thin to X-ray radiation. Mathews & Ferland also point out some problems with the dynamics of the BLR clouds in the hot intercloud medium and conclude that the two-phase picture for the BLR has to be modified to be consistent with the observed emission line and radiation field properties of AGN. Some of the problems of the two-phase model may be solved by considering that BLR clouds are part of an outflow (see e.g. Elvis 2000). An outflowing warm wind (with typical temperature of 10^6 K) with embedded cooler clouds does not suffer from the shear stress problems of fast-moving clouds in a stationary hot atmosphere (typical of the two-phase model), and a geometrically thin wind also largely avoids the Compton depth problem pointed out by Mathews & Ferland (1987). The structure of the Krolik et al. (1981) multiphase medium is then retained rather than abandoned, but many of the problems arising from the presence of an extended, static, hot confining medium are solved quite naturally mostly thanks to the dynamical nature of the outflowing solution. Hence, outflow models for the BLR have received considerable attention in the last decade. Below, we discuss the implications of our observational results on GSN 069 for outflow-based models of the BLR in AGN.

9.2 The BLR as part of a disc-wind

The inability of some AGN to form the BLR is theoretically predicted by several models, mostly based on the idea that the BLR is part of an outflow, or disc-wind (Emmering et al. 1992; Murray et al. 1995; Elvis 2000; Nicastro 2000; Elitzur & Ho 2009 and references therein). We discuss here the implications of our observational data for models associating the BLR with AGN outflows. In the discussion below, we assume the best-fitting parameters of our pure AD model, i.e. $M_{\rm BH} = 1.2 \times 10^6\,{\rm M}_\odot$ and $\lambda = 0.5$. Moreover we assume the standard accretion efficiency $\eta = 0.06$ for a non-rotating black hole, and a viscosity parameter $\alpha = 0.1$.

For the above parameters, all available models predict that GSN 069 should have developed a disc-outflow already. If the BLR are associated with disc-winds, broad emission lines should then be present, contrary to our optical spectroscopic observations. On the other hand, $\lambda^{\rm hist} \sim 2 \times 10^{-2}$, as inferred from the NLR line luminosity. Such lower Eddington ratio may be insufficient to give rise to a disc-wind and, moreover, it may be associated with a different accretion flow geometry comprising, for instance, a radiatively inefficient inner part (hereafter called RIAF for simplicity, e.g. Begelman, Blandford & Rees 1984; Narayan, Yi & Mahadevan 1995; Yuan 2007), and a standard outer disc. In fact, most models predict that the transition between a disc–RIAF solution and a disc-only one occurs around $\lambda \simeq 10^{-2}$ (or even above, see e.g. Rozanska & Czerny 2000, where the transition to an inner RIAF solution is predicted to occur at $\sim 7 \times 10^{-2}$ in AGN for $\alpha \simeq 0.1$). If GSN 069 was in the past characterized by an RIAF–disc flow, a standard disc-wind may have developed only recently, following a relatively recent re-activation of GSN 069, i.e. a transition from a radiatively inefficient RIAF–disc to a radiatively efficient disc-only solution, only the latter being associated with a disc-wind.

9.2.1 *BLR formation time-scale in disc-wind models*

The state transition from an RIAF–disc to a disc-only accretion mode must have occurred some time before 2007, as the *GALEX* data indicate a high radiative efficiency at that epoch (see Fig. 6). This would imply that, if the BLR forms via a disc-wind, its formation time-scale is longer than $\sim$3 yr, i.e. the time-span between the *GALEX* observation in 2007, when GSN 069 already had a high $\lambda \gtrsim 0.5$ (see Fig. 6), and the AAT optical spectrum in 2010, where no evidence for a BLR is found. Is a $\sim$3 yr minimum BLR formation time-scale consistent with a disc-wind origin of the BLR? Once the launching/accelerating conditions are met, an outflow should be launched instantly (light-travel time affects are totally negligible here), so the answer appears to be negative.

Let us, however, consider a general geometry of radiatively-driven disc-wind models in some more detail. The wind is expected to initially rise vertically at $R_{\rm wind}$ with velocity v_0. As shown by Risaliti & Elvis (2010) and Nomura et al. (2013) based on non-hydrodynamical models, the wind likely comprises three main zones: an inner failed wind which is too ionized (or too dense in the Nomura et al. 2013 study) to be efficiently radiatively accelerated; a middle zone (typically with launching radii of the order of hundreds of r_g) where ionization is relatively low so that the gas is efficiently radiatively accelerated up to escape velocity; an outer zone where the local disc luminosity and the UV irradiation from the innermost regions are weak, so that the wind never reaches escape velocity and fails (or it is not even launched vertically).

According to this simple geometry, the inner zone represents the so-called shielding gas (e.g. Murray et al. 1995, see also Proga, Stone & Kallman 2000) which reduces the ionization of the outer zones; the middle zone gives rise to the actual disc-wind, which is observationally identified with the broad, blueshifted high-ionization-emission-lines (HIEL) such as e.g. C IV, and with the corresponding absorption-lines whenever our LOS crosses the wind itself as in narrow/broad-absorption-lines AGN. On the other hand, the outermost failed wind may be responsible for some of the lowerionization broad emission lines (e.g. the Blamer lines as well as Mg II) which are generally symmetric and centred at rest-frame

wavelength. The observational evidence that the low–ionization-emission-lines (LIEL) see a continuum that has been filtered through the wind (e.g. Leighly 2004; Leighly & Moore 2004) provides further support to this geometry for the BLR, which is often referred to as the wind–disc geometry of the BLR, to differentiate the two main BLR regions, of which one is dominated by outflows, the other by gravity (e.g. Richards et al. 2011 and references therein).

As our AAT observation only could target the LIEL, we are here concerned with the so-called disc component of the BLR only. In order for the gas to produce the LIEL, substantial EUV and soft X-rays irradiation is required. However, all disc-wind models (e.g. Risaliti & Elvis 2010; Nomura et al. 2013) and simulations (e.g. Proga & Kallman 2004, see also subsequent work by Schurch, Done & Proga 2009 and by Sim et al. 2010) demonstrate that soft X-rays and EUV irradiation is weak close to the disc plane at relatively large radii because of absorption and Compton scattering in the inner wind/shield, and because of the angular dependence of the disc emission itself. In fact, one can qualitatively infer that zones within $i_{\rm crit} \sim 25^{\circ}$ from the disc plane are unlikely to be efficiently irradiated. Hence, any wind (either accelerated or failed) has to initially rise vertically to a height $z \sim \tan(i_{\rm crit}) R_{\rm wind} \sim 0.5 R_{\rm wind}$ in order to be exposed to sufficient irradiation to produce the LIEL. The rising time is obviously $\Delta t \sim 0.5 R_{\rm wind} v_0^{-1}$, where v_0 is the vertical rising velocity.

We can then estimate the minimum launching radius $R_{\rm wind}^{\rm (min)}$ that is consistent with the observationally derived minimum LIEL–BLR formation time-scale of $\sim$3 yr for GSN 069. Assuming, for simplicity, that $v_0 = 10^2\,{\rm km\,s^{-1}}$ at all radii (Risaliti & Elvis 2010), $R_{\rm wind}^{\rm (min)} \sim 1.9 \times 10^{15}$ cm$\sim 10^4 r_g$. If the wind is launched from $R_{\rm wind} \gtrsim R_{\rm wind}^{\rm (min)}$ the LIEL–BLR formation time-scale is longer than $\sim$3 yr and thus consistent with the GSN 069 data. It is interesting to compare this value with the BLR radius, as derived from the BLR size–luminosity relation (e.g. Kaspi et al. 2005; Bentz et al. 2006) which suggests $R_{\rm BLR} \sim 1.2 \times 10^{16}$ cm in GSN 069. Reassuringly, $R_{\rm BLR}$ is significantly larger than $R_{\rm wind}^{\rm (min)}$.

We point out here that $R_{\rm wind}^{\rm (min)} \sim 10^4 r_g$ is much larger than the typical radius where disc-winds can be launched vertically due to the local radiation pressure (see e.g. Nomura et al. 2013). Moreover, any disc-wind launched and accelerated within $\sim 500 r_g$ to escape velocity, would reach $R_{\rm BLR}$ in less than a year, thus predicting much shorter LIEL–BLR formation time-scales than observed ($\gtrsim$3 yr). We can conclude that the LIEL are not formed directly in the standard disc-wind launched at hundreds of r_g from the central black hole.

Our results are instead consistent with the idea proposed by Czerny & Hryniewicz (2011) in which the LIEL–BLR originate in a dust-driven outflow launched off the disc between the radius $R_{1000\rm K}$ where the local temperature is $\sim$1000 K (i.e. dust can survive within the disc), and the dust sublimation radius $R_{\rm dust}$. Czerny & Hryniewicz (2011) show that $R_{1000\rm K} \simeq R_{\rm BLR}$ in objects where $R_{\rm BLR}$ has been measured via reverberation mapping, so that their idea has a sound observational basis. The presence of dust in this range of radii boosts the effect of radiation pressure with respect to the case of a dust-free gas, and contributes to drive a massive vertical outflow off the disc. When the gas reaches sufficiently high elevation to be irradiated, it loses any dust content and the outflow fails (as at these large radii irradiation is not strong enough to drive a radial wind, see e.g. Risaliti & Elvis 2010). Such dynamics, comprising rising and falling clumps, provides a turbulent medium dominated by Keplerian motion, an elegant description of what the LIEL–BLR may indeed look like. Moreover, the outer parts of the dust-driven wind beyond the dust sublimation radius may give rise to the so-called obscuring torus which is likely outflowing due to the radiation pressure on the dust grains, linking the BLR and the torus structures via a unique dust-driven outflow.

Within this model, a dust-driven wind rising vertically from $R_{\rm BLR} \simeq R_{1000\rm K}$ with velocity $v_0 \sim 10^2$ km s^{-1} would be irradiated after $\sim$20 yr in GSN 069, hence the LIEL will start to form within about 20 yr of the re-activation of GSN 069. However, for the LIEL lines to be detected, the irradiated gas needs to reach a substantial filling factor. Assuming that a standard BLR comprises the whole region between $R_{1000\rm K}$ and $R_{\rm dust}$, a fully mature LIEL–BLR in GSN 069 may take a few hundreds of years to develop, although weak LIEL may start to be visible a few tens of years after the re-activation.

9.2.2 *On the wind component of the BLR*

As discussed above, the lack of broad LIEL in GSN 069 is consistent with an outflow origin, provided that the wind is launched further away than $R_{\rm wind}^{\rm (min)} \sim 1.9 \times 10^{15}$, possibly indicating a dust-driven wind origin for the disc component of the BLR, as suggested by Czerny & Hryniewicz (2011). However, an inner disc-wind should have been launched in GSN 069 already, giving rise to potentially observable broad and blueshifted HIEL such as e.g. C IV. Future spectroscopic UV observations of GSN 069 may then reveal the presence of such a wind component which, being launched from smaller radii, is already exposed to UV irradiation and should reveal itself as a HIEL emitter. Observations targeting simultaneously both the wind (C IV) and the disc (Mg II) component of the BLR may therefore be crucial for our understanding of the overall (wind and disc) BLR formation mechanisms and time-scales. A simple sketch of the envisaged geometry of the system within the disc-wind (and dust-driven wind) scenario is presented in Fig. 7.

10 SUMMARY AND CONCLUSIONS

GSN 069 can be classified as a Seyfert 2 galaxy in the optical. The lack of cold X-ray absorption as well as the soft X-rays short time-scale variability rule out a standard Seyfert 2 galaxy interpretation of the X-ray data, suggesting that GSN 069 is a true Seyfert 2 galaxy candidate which lacks the BLR (or has very weak lines). The source is undetected above 1 keV, suggesting a particularly weak (or absent) optically thin standard X-ray corona resulting in a very large 2–10 keV Bolometric correction $\geq$1800. The X-ray spectrum is affected by warm absorption and it is significantly softer than the typical AGN soft excess. It can be described by pure AD thermal emission suggesting a black hole mass of $\sim 1.2 \times 10^6\,{\rm M_{\odot}}$ and Eddington ratio $\lambda \sim 0.5$ ($L_{\rm Bol} \sim 8 \times 10^{43}$ erg s^{-1}). The historical Bolometric luminosity, as traced by the NLR emitting gas, is instead $\sim 3 \times 10^{42}$ erg s^{-1}, thus corresponding to a historical Eddington ratio of $\lambda^{\rm hist} \sim 2 \times 10^{-2}$. Although spectropolarimetric observations would be needed to exclude the presence of an HBLR, GSN 069 appears to be a puzzling true Seyfert 2 galaxy candidate with higher-than-critical Eddington ratio for the BLR disappearance (i.e. for the disc-wind disappearance according to Nicastro 2000; Trump et al. 2011). We propose two possible scenarios that can explain our observations.

In the first scenario, the lack of optical broad lines in GSN 069 is directly linked with the lack of hard X-rays. This is because, if the BLR consists of relatively cold clouds in pressure equilibrium with a much hotter inter-cloud medium, the lack of hard X-ray emission implies a dramatic drop of the Compton temperature of the gas,

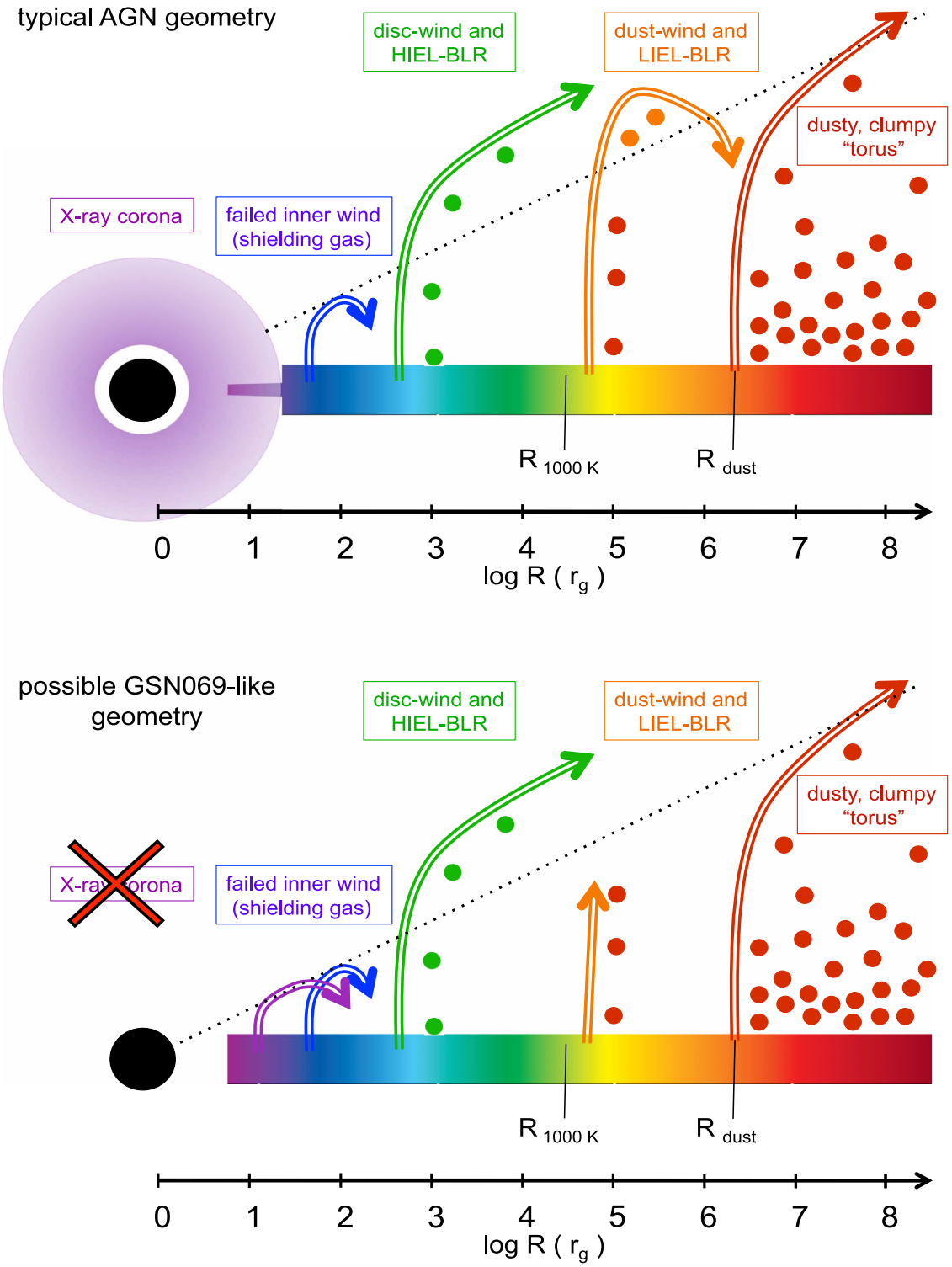

Figure 7. In the upper panel, we present a schematic view of the possible disc-wind/BLR/torus typical geometry. The dotted line shows the radial direction with $i_{\rm crit} = 25^{\circ}$ from the disc plane. We assume that shielding is provided by an inner failed-wind. A standard disc-wind launched at hundreds of r_g produces the HIEL, while a failed dust-driven wind is responsible for the LIEL at larger radii. In the lower panel, we show one possible geometry for GSN 069. The inner failed wind (i.e. the shielding gas) may extend to inner radii disrupting the corona. The dust-driven wind is not yet irradiated, its motion is purely vertical, and no LIEL–BLR is formed yet. Whether a disc-wind producing the HIEL is already present could be clarified with future UV spectroscopic observations.

destroying the two-phase stability regime of the cloud/intercloud medium, Hence, although the EUV and soft X-rays luminosity is high enough to produce the optical emission lines, the extreme hard X-ray weakness of GSN 069 prevents the BLR from reaching the necessary two-phase equilibrium, leading to the suppression of the line-emitting region thermodynamically. Such idea may be tested by following the evolution (if any) of the hard X-ray emission in GSN 069 and similar objects (e.g.2XMM J123103.2+110648 which has

similar properties and also lacks hard X-ray emission). The detection of sources with a standard level of hard X-ray emission but with no BLR would challenge the idea of a two-phase component for the BLR, and would imply that this interpretation is unlikely to be viable in GSN 069. Bianchi et al. (2012) point out the existence of two such candidates (Mrk 273x and 1ES 1927+654) which are surely worth further study.

In the second scenario, GSN 069 has recently experienced a transition from a relatively radiatively inefficient state ($\lambda^{\rm hist} \sim 2 \times 10^{-2}$) to a highly efficient one ($\lambda \sim 0.5$, likely already in place during the 2007 *GALEX* observation). A disc-wind has then formed recently following this re-activation, and its signature may be revealed by looking for broad and blueshifted HIEL (e.g. C IV) in future UV spectroscopic observations. As for the LIEL, our data can be used to infer a minimum LIEL–BLR formation time-scale of $\geq$3 yr which is consistent with the idea of a dust-driven wind launched at $R_{\rm wind} \gtrsim 1.9 \times 10^{15}$ cm (consistent with the estimated $R_{\rm BLR} \sim 1.2 \times 10^{16}$ cm). The dust-driven outflow is then still in its rising phase, so that no LIEL are formed yet. The lines form when the dusty-wind begins to be irradiated (a few tens of years after it has been launched), although it will take about one order of magnitude more time to form a fully mature LIEL–BLR filling the entire BLR region out to the dust sublimation radius. On the other hand, our results seem to rule out that the LIEL are part of a standard disc-wind launched at few hundreds of r_g, as the wind would already have reached the BLR typical location producing broad optical lines, in contrast with the minimum $\sim$3 yr time-scale we derive observationally. Within the latter, outflow-based scenario, the lack of hard X-ray emission in GSN 069 (and 2XMM J123103.2+110648, see also the case of RX J1301.9+2747, recently reported by Sun, Shu & Wang 2013) could be associated with a very early phase in the transition from a radiatively inefficient to an efficient flow. It is possible that an inner failed wind is present at this evolutionary stage, quenching the formation of a standard X-ray corona which may settle down into its optically thin configuration later on (e.g. Proga 2005).

It is also worth mentioning that the model of episodic BLR formation proposed by Wang et al. (2012) in the context of star-forming, self-gravitating discs in AGN predicts the existence of a (rare) population of so-called Panda AGN that should exhibit relatively high Eddington ratio with no BLR signatures during the early stages of the BLR formation. Although the lifetime of such a phase may be very short in GSN 069 (primarily due to the low black hole mass), it is interesting to note that GSN 069 may represent one Panda AGN candidate, to be confirmed with future spectropolarimetric, as well as UV spectroscopic observations.

Finally, it is interesting to note that GSN 069 (and 2XMM J123103.2+110648) may represent (one of) the long-sought missing links between black hole X-ray binaries and supermassive accreting black holes. Indeed, the properties of GSN 069 suggest that this AGN is currently in a super-soft state, similar to that experienced by some black hole X-ray transients during their outburst evolution, when the emission is completely dominated by the AD thermal emission, and the hard X-ray contribution to the Bolometric luminosity is negligible. GSN 069 was here detected and classified properly only thanks to its small black hole mass and high Eddington ratio, which shifts the AD thermal emission up to the soft X-rays. AGN powered by larger black holes and/or accreting at lower rates would not have been detected in the soft X-rays at all. It is then possible that there is an entire population of AGN with more typical (larger) black hole mass in super-soft states that are completely missed in current X-ray surveys. A GSN 069-like object with larger black hole mass would in fact be likely classified as a Compton-thick candidate. Assuming typical Eddington ratio $\lambda = 0.1$ (and non-rotating black holes), no soft X-rays are expected from the AD thermal emission for $M_{\rm BH} \geq$ few $\times 10^7$ M$_\odot$ at redshift zero, so that almost all GSN 069-like AGN would be misclassified as Compton-thick type 2 candidates in even moderately high-redshift surveys. If the population of GSN 069-like objects with typical 10^7-10^8 M$_\odot$ black hole mass is not negligible, these sources may then contaminate the fraction of heavily obscured AGN in the Universe as derived from current X-ray surveys. Moreover, if the analogy with black hole binaries holds, the life-time of super-soft states in AGN could be as long as 10^4-10^5 yr, i.e. orders of magnitude longer than the time X-ray observatories have existed. As such, we cannot exclude that the fraction of GSN 069-like, super-soft AGN is not negligible in the Universe. Future studies will be devoted to assess the relevance of GSN 069-like objects for the overall AGN population.

ACKNOWLEDGEMENTS

Based on observations obtained from *XMM–Newton*, an ESA science mission with instruments and contributions directly funded by ESA Member States and NASA. This work made use of data supplied by the UK Swift Science Data Centre at the University of Leicester. This publication makes use of data products from the *Wide-field Infrared Survey Explorer* (*WISE*), which is a joint project of the University of California, Los Angeles, and the Jet Propulsion Laboratory/California Institute of Technology, funded by the National Aeronautics and Space Administration. We also made use of data from the NASA *Galaxy Evolution Explorer* (*GALEX*), operated for NASA by the California Institute of Technology under NASA contract NAS5-98034, as well as of data from the Two Micron All Sky Survey (2MASS), a joint project of the University of Massachusetts and the Infrared Processing and Analysis Center/California Institute of Technology, funded by the National Aeronautics and Space Administration and the National Science Foundation. We thank the anonymous referee for constructive criticism and suggestions that significantly helped us to improve our paper. GM also thanks Margherita Giustini and Sara Motta for valuable discussions. GM and PE acknowledge support from the Spanish Plan Nacional de Astronomía y Astrofísica under grants AYA2010-21490-C02-02 and AYA2009-05705-E, respectively. AMR acknowledges UKSA funding support.

REFERENCES

Antonucci R., 1993, ARA&A, 31, 473
Antonucci R., 2012, Astron. Astrophys. Trans., 27, 557
Baldwin J. A., Phillips M. M., Terlevich R., 1981, PASP, 93, 5
Begelman M. C., Blandford R. D., Rees M. J., 1984, Rev. Mod. Phys., 56, 255
Bentz M. C., Peterson B. M., Pogge R. W., Vestergaard M., Onken C. A., 2006, ApJ, 644, 133
Bian W., Gu Q., 2007, ApJ, 657, 159
Bianchi S. et al., 2012, MNRAS, 426, 3225
Brightman M., Nandra K., 2008, MNRAS, 390, 1241
Bruzual G., Charlot S., 2003, MNRAS, 344, 1000
Crummy J., Fabian A. C., Gallo L., Ross R. R., 2006, MNRAS, 365, 1067
Czerny B., Hryniewicz K., 2011, A&A, 525, L8
Done C., Davis S. W., Jin C., Blaes O., Ward M., 2012, MNRAS, 420, 1848
Dong R., Greene J. E., Ho L. C., 2012, ApJ, 761, 73
Dunn R. J. H., Fender R. P., Körding E. G., Belloni T., Cabanac C., 2010, MNRAS, 403, 61
Elitzur M., 2012, ApJ, 747, L33

Elitzur M., Ho L. C., 2009, ApJ, 701, L91
Elitzur M., Shlosman I., 2006, ApJ, 648, L101
Elvis M., 2000, ApJ, 545, 63
Emmering R. T., Blandford R. D., Shlosman I., 1992, ApJ, 385, 460
Esquej P. et al., 2008, A&A, 489, 543
Filippenko A. V., Sargent W. L. W., 1988, ApJ, 324, 134
Greene J. E., Ho L. C., 2004, ApJ, 610, 722
Greene J. E., Ho L. C., 2005, ApJ, 630, 122
Greene J. E., Ho L. C., 2007, ApJ, 670, 92
Guilbert P. W., McCray R., Fabian A. C., 1983, ApJ, 266, 466
Hernán-Caballero A., Hatziminaoglou E., 2011, MNRAS, 414, 500
Ho L. C., 2008, ARA&A, 46, 475
Ho L. C., Filippenko A. V., Sargent W. L. W., 1997, ApJS, 112, 315
Ho L. C., Kim M., Terashima Y., 2012, ApJ, 759, L16
Jin C., Ward M., Done C., Gelbord J., 2012, MNRAS, 420, 1825
Just D. W., Brandt W. N., Shemmer O., Steffen A. T., Schneider D. P., Chartas G., Garmire G. P., 2007, ApJ, 665, 1004
Kalberla P. M. W., Burton W. B., Hartmann D., Arnal E. M., Bajaja E., Morras R., Pöppel W. G. L., 2005, A&A, 440, 775
Kaspi S., Maoz D., Netzer H., Peterson B. M., Vestergaard M., Jannuzi B. T., 2005, ApJ, 629, 61
Krolik J. H., McKee C. F., Tarter C. B., 1981, ApJ, 249, 422
Lamastra A., Bianchi S., Matt G., Perola G. C., Barcons X., Carrera F. J., 2009, A&A, 504, 73
Leighly K. M., 2004, ApJ, 611, 125
Leighly K. M., Moore J. R., 2004, ApJ, 611, 107
Marconi A., Hunt L. K., 2003, ApJ, 589, L21
Marinucci A., Bianchi S., Nicastro F., Matt G., Goulding A. D., 2012, ApJ, 748, 130
Mathews W. G., 1974, ApJ, 189, 23
Mathews W. G., Ferland G. J., 1987, ApJ, 323, 456
McKee C. F., Tarter C. B., 1975, ApJ, 202, 306
Metcalfe N., Fong R., Shanks T., Kilkenny D., 1989, MNRAS, 236, 207
Miniutti G., Ponti G., Greene J. E., Ho L. C., Fabian A. C., Iwasawa K., 2009, MNRAS, 394, 443
Murray N., Chiang J., Grossman S. A., Voit G. M., 1995, ApJ, 451, 498
Narayan R., Yi I., Mahadevan R., 1995, Nat, 374, 623
Nicastro F., 2000, ApJ, 530, L65
Nikolajuk M., Papadakis I. E., Czerny B., 2004, MNRAS, 350, L26
Nomura M., Ohsuga K., Wada K., Susa H., Misawa T., 2013, PASJ, 65, 40
Panessa F., Bassani L., 2002, A&A, 394, 435
Panessa F. et al., 2009, MNRAS, 398, 1951
Pappa A., Georgantopoulos I., Stewart G. C., Zezas A. L., 2001, MNRAS, 326, 995
Peimbert M., Torres-Peimbert S., 1981, ApJ, 245, 845
Piconcelli E., Jimenez-Bailón E., Guainazzi M., Schartel N., Rodríguez-Pascual P. M., Santos-Lleó M., 2005, A&A, 432, 15
Ponti G., Papadakis I., Bianchi S., Guainazzi M., Matt G., Uttley P., Bonilla N. F., 2012, A&A, 542, A83
Proga D., 2005, ApJ, 630, L9
Proga D., Kallman T. R., 2004, ApJ, 616, 688
Proga D., Stone J. M., Kallman T. R., 2000, ApJ, 543, 686
Reeves J., Done C., Pounds K., Terashima Y., Hayashida K., Anabuki N., Uchino M., Turner M., 2008, MNRAS, 385, L108
Remillard R. A., McClintock J. E., 2006, ARA&A, 44, 49
Richards G. T. et al., 2011, AJ, 141, 167
Risaliti G., Elvis M., 2010, A&A, 516, A89
Rozanska A., Czerny B., 2000, A&A, 360, 1170
Saunders W. et al., 2004, in Moorwood A. F. M., Masanori I., eds, Proc. SPIE Vol. 5492, Ground-based Instrumentation for Astronomy. SPIE, Bellingham, p. 389
Saxton R., Read A., Esquej P., Miniutti G., Alvarez E., 2011, in Foschini L., Colpi M., Gallo L., Grupe D., Komossa S., Leighly K., Mathur S., eds, Proc. Sci. Vol. NLS1, Narrow-Line Seyfert 1 Galaxies and their Place in the Universe, avaliable at http://pos.sissa.it/cgi-bin/reader/conf.cgi?confid=126, id.8 (arXiv:1106.3507)
Saxton R. D., Read A. M., Esquej P., Komossa S., Dougherty S., Rodriguez-Pascual P., Barrado D., 2012, A&A, 541, A106
Schurch N. J., Done C., Proga D., 2009, ApJ, 694, 1
Sharp R., Birchall M. N., 2010, Publ. Astron. Soc. Aust., 27, 91
Sharp R. et al., 2006, in McLean I. S., Masanori I., eds, Proc. SPIE Vol. 6269, Ground-based and Airborne Instrumentation for Astronomy. SPIE, Bellingham, p. 62690G
Shi Y., Rieke G. H., Smith P., Rigby J., Hines D., Donley J., Schmidt G., Diamond-Stanic A. M., 2010, ApJ, 714, 115
Sim S. A., Proga D., Miller L., Long K. S., Turner T. J., 2010, MNRAS, 408, 1396
Stern J., Laor A., 2012, MNRAS, 426, 2703
Sun L., Shu X., Wang T., 2013, ApJ, 768, 167
Terashima Y., Kamizasa N., Awaki H., Kubota A., Ueda Y., 2012, ApJ, 752, 154
Tran H. D., 2003, ApJ, 583, 632
Trump J. R. et al., 2011, ApJ, 733, 60
Vasudevan R. V., Mushotzky R. F., Winter L. M., Fabian A. C., 2009, MNRAS, 399, 1553
Veilleux S., Osterbrock D. E., 1987, ApJS, 63, 295
Wang J.-M., Zhang E.-P., 2007, ApJ, 660, 1072
Wang J.-M., Du P., Baldwin J. A., Ge J.-Q., Hu C., Ferland G. J., 2012, ApJ, 746, 137
Wolfe A. M., 1974, ApJ, 188, 243
Wu Y.-Z., Zhang E.-P., Liang Y.-C., Zhang C.-M., Zhao Y.-H., 2011, ApJ, 730, 121
Xiao T., Barth A. J., Greene J. E., Ho L. C., Bentz M. C., Ludwig R. R., Jiang Y., 2011, ApJ, 739, 28
Yuan F., 2007, in Ho L. C., Wang J.-M., eds, ASP Conf. Ser. Vol. 373, The Central Engine of Active Galactic Nuclei. Astron. Soc. Pac., San Francisco, p. 95

This paper has been typeset from a TEX/LATEX file prepared by the author.